Cellular and Molecular Biology

Original Article

Bone mesenchymal stem cell-derived exosomal miR-26a-3p promotes autophagy to attenuate LPS-induced apoptosis and inflammation in pulmonary microvascular endothelial cells

Qianfei Wang*, Yiming Huang, Zherui Fu

Department of Emergency, The First People's Hospital of Xiaoshan District, Hangzhou, Hangzhou, 311200, Zhejiang, China

Article Info

Abstract

Acute lung injury (ALI) is a serious lung disease. The apoptosis and inflammation of pulmonary microvascular endothelial cells (PMVECs) are the primary reasons for ALI. This study aimed to explore the treatment effect and regulatory mechanism of bone mesenchymal stem cell-derived exosomes (BMSC-expos) on ALI. PMVECs were stimulated by Lipopolysaccharide (LPS) to imitate ALI environment. Cell viability was determined by CCK-8 assay. Cell apoptosis was evaluated by TUNEL and flow cytometry. ELISA was utilized for testing the contents of TNF-α, IL-1β, IL-6, and IL-17. Western blot was applied for testing the levels of autophagy-related proteins LC3, p62, and Beclin-1. RNA interaction was determined by luciferase reporter assay. The ALI rat model was established by intratracheal injection of LPS. Evans blue staining was utilized for detecting pulmonary vascular permeability. Our results showed that LPS stimulation notably reduced cell viability, increased cell apoptosis rate, and enhanced the contents of inflammatory factors in PMVECs. However, BMSC-exo treatment significantly abolished the promoting effects of LPS on cell injury. In addition, we discovered that BMSC-exo treatment notably activated autophagy in LPS-induced PMVECs. Furthermore, BMSC-expos upregulated miR-26a-3p expression and downregulated PTEN in PMVECs. MiR-26a-3p was directly bound to PTEN. MiR-26a-3p overexpression reduced cell apoptosis, and inflammation and promoted autophagy by silencing PTEN. Animal experiments proved that miR-26a-3p overexpression effectively improved LPS-induced lung injury in rats. The results proved that BMSC-expos promotes autophagy to attenuate LPS-induced apoptosis and inflammation in pulmonary microvascular endothelial cells via miR-26a-3p/PTEN axis.

Keywords: Bone marrow mesenchymal stem cells, Exosome, MiR-26a-3p, PTEN, Pulmonary microvascular endothelial cells

1. Introduction

Acute lung injury (ALI) is a serious lung disease, often accompanied by pulmonary microvascular leakage, pulmonary edema, pleural effusion, and diffuse alveolar injury, leading to high mortality rates [1]. The alveolar-capillary barrier is formed by pulmonary microvascular endothelial cells (PMVECs), and it is vital for gas exchange and preventing fluid leakage. The main pathological features of ALI are the inflammatory response and cell apoptosis of damaged PMVECs, which increase the permeability of pulmonary microvascular endothelium, resulting in pulmonary edema and alveolar collapse [2]. ALI is caused by various factors, with pathogenic infections such as sepsis being the main cause. Lipopolysaccharide (LPS) is one of the main toxic components of the outer membrane of Gram-negative bacteria, and it has been found to cause ALI through the induction of inflammatory response [3]. Researches have shown that LPS stimulates PMVECs to cause cell damage and barrier dysfunction, resulting in excessive leakage of protein-rich edema fluid

and accumulation of inflammatory cells in alveolar spaces, ultimately causing pulmonary edema. Therefore, a deep understanding of the mechanisms regulating the function of PMVECs is crucial for developing effective ALI treatment methods.

Bone marrow mesenchymal stem cells (BMSCs) are non-hematopoietic stem cells in the bone marrow that possess the capability to self-renew and differentiate [4]. Due to its ability to create a microenvironment conducive to the repair and regeneration of injured tissues, BMSCs are considered a research hotspot in the field of stem cell therapy. A flow of researches have demonstrated that BMSC transplantation exerts therapeutic effects through paracrine function. Exosomes can be secreted by almost all types of cells and are small membrane vesicles with a diameter of 50-150 nm [5]. They participate in intercellular communication and signal transduction by transferring bioactive molecules, including mRNA, microRNA (miRNA), DNA, lipids, and proteins [6]. Exosomes have been shown to exert vital functions in tissue repair, mo-

---

dulating cell apoptosis, inflammation, and autophagy [7]. Accumulating researches have confirmed that exosomes derived from BMSCs (BMSC-expos) have a wide range of therapeutic effects in different diseases [8], including ALI. For example, BMSC-expos ameliorate acute respiratory distress syndrome via suppressing glycolysis in macrophages. BMSC-expos regulate autophagy to attenuate LPS-induced ALI by upregulating miR-384-5p [9]. However, the functionality of BMSC-expos in ALI needs further exploration.

MiRNA is a small non-coding RNA molecule that exerts momentous functions in various biological processes [10]. They modulate target mRNAs via suppressing translation or facilitating degradation. The dysregulated miRNAs have been found to be closely associated with inflammatory diseases, metabolic diseases, and tumorigenesis. Multiple differentially expressed miRNAs have been identified in ALI and confirmed to take part in modulating ALI development. For example, miR-29a-3p improves ALI via decreasing alveolar epithelial cell PANoptosis [11]. MiR-221-5p reduces the expression of JNK2 to aggravate ALI [12]. MiR-26a-3p has been confirmed to be expressed in the brains and is associated with neuropsychiatric disorders [13]. Wang *et al*. [14] suggest miR-26a-3p depletion is conducive to inflammation in hippocampus by regulating p38 MAPK pathway. In addition, miR-26a-3p can regulate the malignant development of several cancers [15]. Studies have indicated that miRNAs carried by exosomes mediate intercellular signal transduction to influence biological functions of donor cells on recipient cells in assorted diseases [16]. It is reported that exosomal miR-150 attenuates ALI progression by mediating the function of PMVECs via MAPK pathway [17]. Nevertheless, the roles of exosomal miR-26a-3p derived from BMSCs in ALI are still rarely explored.

This study primarily explored the effects of BMSC-expos and miR-26a-3p on the progression of ALI. We hypothesized that BMSC-expos may regulate LPS-mediated cell apoptosis, inflammation, and autophagy by delivering exosomal miR-26a-3p to PMVECs, thereby affecting ALI development.

2. Materials and methods
2.1. Cell culture
PMVECs and BMSCs were obtained from Procell Biotechnology Co., Ltd (Wuhan, China). BMSCs were incubated in LG-DMEM (Gibco, USA) containing 10% FBS and 1% P/S. PMVECs were cultured in an endothelial growth medium (Procell) at 37°C with 5% CO_2. PMVECs were treated with 100 ng/mL LPS (Sigma-Aldrich, USA) for 24 h for imitating the ALI environment.

2.2. Cell transfection
The miR-26a-3p mimics and negative control (NC) mimics are synthesized through Ribobio (Guangzhou, China). The pcDNA3.1-PTEN and empty vector pcDNA3.1 were synthesized through Geenseed Biotech (Guangzhou, China). Lipofectamine 3000 Reagent (Invitrogen) was utilized to perform cell transfection for 48 h.

2.3. RT-qPCR
TRIzol™ reagent (Invitrogen, USA) was utilized for obtaining the total RNA. The RNA was then utilized for reverse transcription by Reverse Transcription Kit (Invi-

trogen). Next, qPCR was performed with QuantiTect SYBR Green RT-PCR Kit (QIAGEN, Germany) on ABI Prism7500 fast real-time PCR system. Gene expression was counted by $2^{-\Delta\Delta Ct}$ method.

2.4. Western blot
The lung tissues or cells were gathered and homogenized in RIPA lysis buffer. Then, the protein samples were separated on 10% SDS-PAGE and then transferred onto PVDF membranes, followed by incubating with primary antibodies (Abcam, USA) at the temperature of 4°C for one night. Then the membranes were rinsed with TBST and incubated with the HRP-conjugated secondary antibody (Abcam) for 2 h. The band density was assessed utilizing an ECL kit (Bio-Rad Laboratories, Shanghai, China).

2.5. Identification of BMSCs
BMSCs were incubated with the osteogenic, adipogenic or chondrogenic differentiation medium (Procell) for three weeks. Then, cells were fixed by 4% PFA and dyed by 1% Alizarin Red S for 5 min to test calcium deposition. Cells were stained with Oil Red O for half an hour to observe lipid droplets. Cells were stained by Alcian Blue staining for half an hour. Immunophenotype of BMSCs was determined through flow cytometry with the fluorescein-conjugated antibodies (anti-CD29, anti-CD44, anti-CD90, anti-CD105, anti-CD11b/c and anti-CD34) in accordance with user guides.

2.6. CCK-8 assay
Cells (4×10^3) were seeded in the 96-well plates and cultured for 48 h. Then, the CCK-8 (Beyotime, Shanghai, China) solution was supplemented into each well for 2 h. The absorbance was assessed with a microplate reader (BioTek Instruments).

2.7. TUNEL assay
A TUNEL assay kit (Roche, USA) was utilized for this assay in accordance with user guides. Cells were subjected to fixation by 4% PFA and permeabilization by 0.2% TritonX-100. Then, they were treated with 50 μL TdT reaction mix for one hour. DAPI was utilized for staining the cell nucleus. The fluorescence microscope (Olympus, Japan) was employed to capture the images.

2.8. Flow cytometry
Annexin-V-FITC apoptosis detection kit (BD Biosciences, USA) was applied for detecting cell apoptotic rate. Cells were treated with 100 μL binding buffer. Annexin V and PI were utilized for staining cells for 10 min without light. The FACS Calibur (BD Biosciences) was applied for analysis.

2.9. ELISA
TNF-α, IL-1β, IL-6, and IL-17 concentrations in cell supernatants were tested by ELISA with their corresponding ELISA Kits (eBioscience, California, USA) in accordance with user guides. The OD value was determined through a microplate reader (BioTek Instruments).

2.10. Isolation and identification of exosomes
Exosomes were extracted from cell supernatant by ultracentrifugation method. Cells and debris were removed through centrifugation at 2000×g for half an hour.

BMSC-expos on ALI

Cell. Mol. Biol. 2024, 70(2): 104-112

Centrifugation at 10 000×g for half an hour was aimed to remove the subcellular component, and centrifugation at 100 000×g for 70 min was aimed to acquire exosomes. In the end, exosomes were subjected to resuspension in 0.01M PBS and centrifugation at 100 000×g for 70 min. Exosomes were identified utilizing a transmission electron microscope (TEM; Philips-Tecnal, Netherlands). The expressions of exosomal biomarkers were assessed through western blot. For the track of exosomes, the Exosome Labeling Kits comprising Exo-red and Exo-green (System Biosciences, USA) were utilized for labeling exosomes.

2.11. Autophagy flux detection

Autophagy flux was evaluated utilizing the mRFP-GFP-LC3 adenovirus transfection assay. Cells were transfected with tandem fluorescent mRFP-GFP-tagged adenovirus (HanBio, China) for 48 h in accordance with user guides. A fluorescence microscope was utilized to obtain the images. Autophagic flux was determined through the color alteration of GFP/mRFP.

2.12. Immunofluorescence (IF) assay

Cells were put in the culture dish and fixed with 4% PFA for half an hour, followed by treatment with 0.2% Triton X-100. After blockading by 5% BSA, cells were cultured with the primary antibodies (Abcam, USA) at the temperature of 4 °C for a whole night. Then they were rinsed with PBS and cultured with secondary antibody for 2 h. DAPI was applied to stain the nucleus. In the end, the images were captured through a fluorescent microscope (Carl Zeiss, Germany).

2.13. Luciferase reporter assay

PTEN 3'UTR fragments containing the binding site with miR-26a-3p were inserted in the pmirGLO luciferase reporter vector (Promega, USA). Cells co-transfected with pmirGLO PTEN 3'UTR luciferase reporter vector and miR-26a-3p mimics or NC mimics with Lipofectamine 3000 (Invitrogen) for 48 h. Dual-Luciferase Reporter Assay System (Promega) was employed for testing luciferase activities.

2.14. RNA pull-down assay

The biotinylated miR-26a-3p was purified and transfected into PMVECs for 48 h. Afterwards, we gathered cells and performed this assay utilizing a Pierce™ Magnetic RNA-Protein Pull-Down Kit (Thermo Fisher Scientific, USA). Cells were lysed and cultured with streptavidin agarose magnetic beads (Thermo Fisher Scientific). The RNA-protein complex was purified utilizing the RNeasy Mini Kit (QIAGEN) and bound RNAs were analyzed through RT-qPCR.

2.15. Animal experiments

All experimental processes endorsed by the First People's Hospital of Xiaoshan District, Hangzhou. Male SD rats (180–220 g) were purchased from The First People's Hospital of Xiaoshan District, Hangzhou and raised for seven days. Rats were randomly divided into three groups (n=10 for each group): the sham group, the LPS group, and the LPS+miR-26a-3p. For establishment of ALI rat model, rats were intratracheally received 5 mg/kg LPS in 50 μl of PBS for 24 h. Rats in the sham group received equal volume PBS. Rats in LPS+miR-26a-3p

group received 80 mg/kg of miR-26a-3p agomiR (Ribo-Bio, Guangzhou, China) through tail vein injection half an hour after injection of LPS. After that, rats were sacrificed and the lungs, bronchoalveolar lavage fluid (BALF), and serum were collected for experiments. For detecting the wet(W)/dry(D) rate, we weighed the lungs and subsequently placed them into a vacuum oven at 58°C until the dry weight was obtained.

2.16. HE staining

Lung tissues were fixed by 4% PFA, dehydrated in ethanol gradient, embedded in paraffin and cut into 5 μm thickness sections. Tissues were then dyed with haematoxylin and eosin for 5 min. A light microscope (Leica) was employed for observation.

2.17. Evans blue dye extravasation assay

Half an hour before the rats were euthanized, we injected 45 mg/kg Evans blue dye (Sigma-Aldrich) into their external jugular veins. Then PBS was utilized to perfuse the lungs to flush the blood. Then, lung samples were homogenized, cultured with 2 volumes of formamide (18 h, 60°C) and centrifuged (12,000 × g, 20 min). Then, we gathered the supernatant and determined the absorbance at 620 nm utilizing a microplate reader.

2.18. Statistical analysis

Statistical analyses were performed by the application of GraphPad Prism 8 software. Data are presented as mean ± SD from 3 individual repeats. The group difference was analyzed with one-way ANOVA or student t-test. $p < 0.05$ was considered significant.

3. Results

3.1. BMSC-expos improve LPS-induced apoptosis and inflammation in PMVECs

For the identification of BMSCs, we performed flow cytometry analysis and discovered that BMSCs positively expressed the specific surface markers of MSCs (CD29, CD44, CD90 and CD105), while negatively expressing CD11b/c, CD34 and CD45 (Figure 1A). After the induction of adipogenic chondrogenic, or osteogenic medium, BMSCs exhibited differentiation to osteogenic, adipogenic, and chondrogenic lineages (Figure 1B). These results confirmed the characterization and differentiation ability of BMSCs. Then, PMVECs were stimulated with LPS for simulating the inflammatory state and CCK-8 assay proved that cell viability was markedly declined under LPS treatment (Figure 1C). Accumulating researches have confirmed that BMSCs can regulate inflammatory response and promote tissue repair by secreting exos [18]. Therefore, we examined the impact of BMSCs on LPS-induced PMVECs activity. BMSCs were co-cultured with PMVECs and then exosome inhibitor GW4869 was supplemented. We discovered that, compared to the LPS group, BMSCs in the LPS+BMSC group showed higher viability, while the increased viability was reduced by GW4869 supplement (Figure 1D). We tested the apoptosis and inflammation of PMVECs in different treatment groups. It was illustrated by TUNEL assay that LPS induction notably increased the ratio of TUNEL-positive cells, while BMSC co-culture reduced the ratio. However, GW4869 supplement could reverse the effect of BMSCs (Figure 1E). Furthermore, flow cytometry illustrated that cell apoptosis rate was increased

BMSC-expos on ALI

Cell. Mol. Biol. 2024, 70(2): 104-112
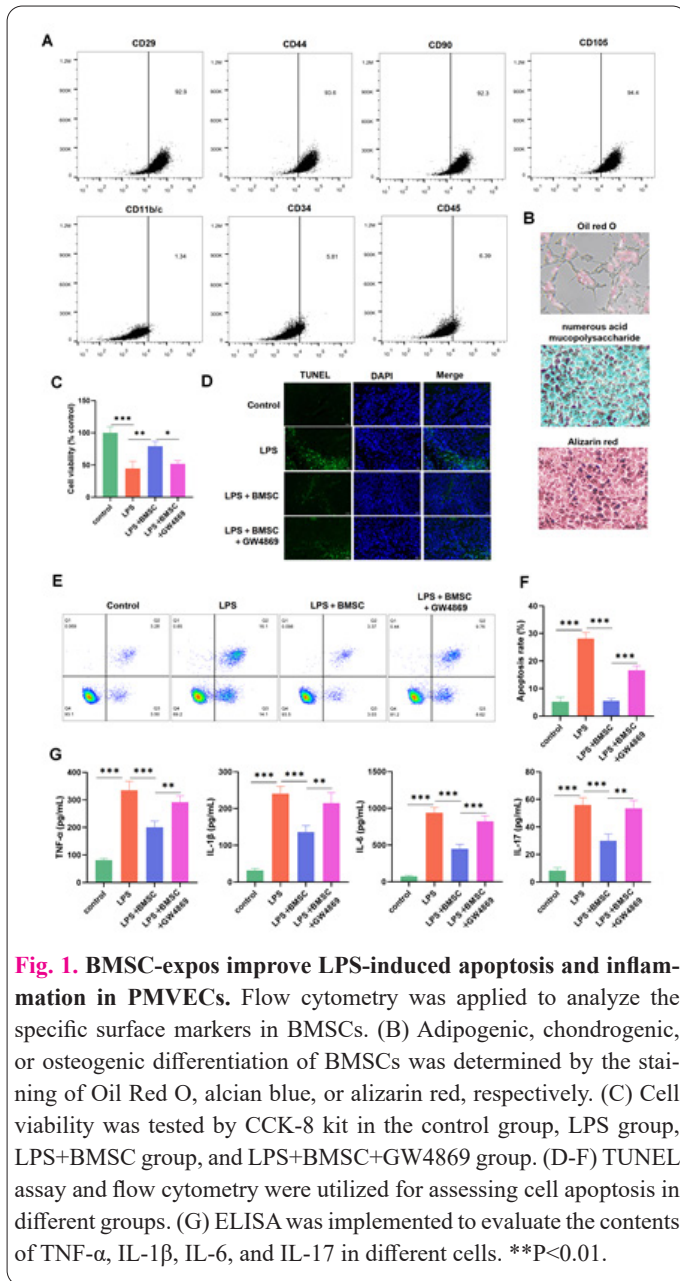
Fig. 1. BMSC-expos improve LPS-induced apoptosis and inflammation in PMVECs. Flow cytometry was applied to analyze the specific surface markers in BMSCs. (B) Adipogenic, chondrogenic, or osteogenic differentiation of BMSCs was determined by the staining of Oil Red O, alcian blue, or alizarin red, respectively. (C) Cell viability was tested by CCK-8 kit in the control group, LPS group, LPS+BMSC group, and LPS+BMSC+GW4869 group. (D-F) TUNEL assay and flow cytometry were utilized for assessing cell apoptosis in different groups. (G) ELISA was implemented to evaluate the contents of TNF-α, IL-1β, IL-6, and IL-17 in different cells. **P<0.01.

by LPS induction. We further observed the decline of cell apoptosis rate in the LPS+BMSC group, and the decrease was counteracted via GW4869 supplement (Figure 1F). Additionally, ELISA outcomes demonstrated that BMSC co-culture reduced the increased contents of TNF-α, IL-1β, IL-6, and IL-17 under LPS induction, while GW4869 treatment reversed the function of BMSCs and recovered their contents in PMVECs (Figure 1G). Thus, we confirmed that exosomes secreted by BMSCs can improve LPS-induced apoptosis and inflammation in PMVECs.

3.2. BMSC-expos activate autophagy in PMVECs

We further investigated the effect of BMSC-expos on autophagy in PMVECs. Firstly, exosomes were extracted from BMSCs via ultracentrifugation and identified by a series of assays. As shown in Figure 2A, the typical spherical exosomes with double-membrane structures were captured under TEM. Then, western blot outcomes illustrated that exosome-specific markers (CD63 and CD9) were markedly expressed in BMSC-expos (Figure 2B). Subsequently, PMVECs were cultured with the labeled Exo-red exosomes or Exo-green exosomes. We observed the intense red and green fluorescence in cells, suggesting

BMSC-expos were taken up by PMVECs (Figure 2C). Then, we explored the impacts of BMSC-expos on autophagy in LPS-stimulated PMVECs. Through TEM, we observed that the LPS treatment notably reduced the quantity of autophagic vacuoles in PMVECs, while BMSC-expos addition reversed the inhibitory function of LPS. After the supplement of autophagy inhibitor 3-MA, the promoting function of BMSC-expos on autophagic vacuoles in LPS-induced PMVECs was notably abolished (Figure 2D). The outcomes of western blot illustrated that LPS stimulation reduced the LC3I/LC3II ratio and Beclin-1 protein levels while increasing p62 level in PMVECs, while BMSC-expos treatment reversed these effects (Figure 2E). Moreover, the autophagy flux of PMVECs was tested utilizing the mRFP-GFP-LC3 adenovirus. We discovered that the formation of autophagosome and autolysosome was restrained in LPS group in comparison to control, suggesting that LPS weakened the autophagy flux in PMVECs. Nevertheless, the addition of BMSC-expos notably increased their formation in LPS-induced cells (Figure 2F). In addition, we proved that 3-MA treatment markedly reversed the functions of BMSC-expos on the alterations of auto-
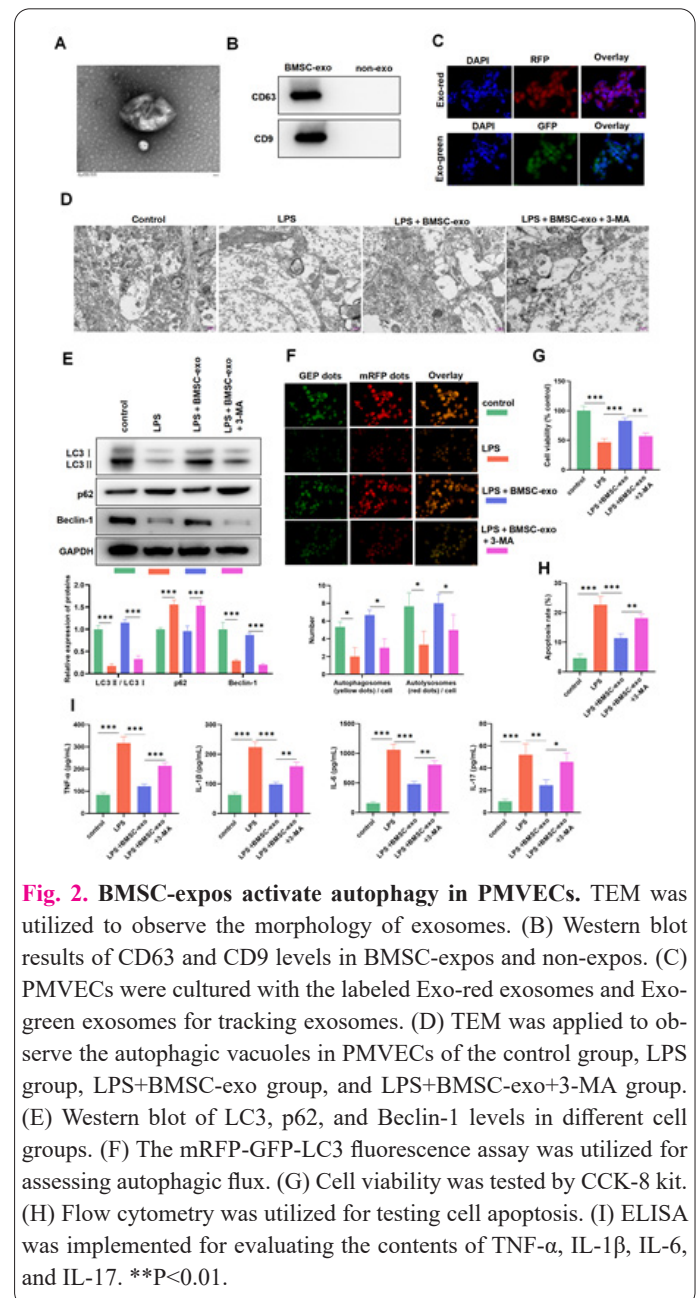
Fig. 2. BMSC-expos activate autophagy in PMVECs. TEM was utilized to observe the morphology of exosomes. (B) Western blot results of CD63 and CD9 levels in BMSC-expos and non-expos. (C) PMVECs were cultured with the labeled Exo-red exosomes and Exo-green exosomes for tracking exosomes. (D) TEM was applied to observe the autophagic vacuoles in PMVECs of the control group, LPS group, LPS+BMSC-exo group, and LPS+BMSC-exo+3-MA group. (E) Western blot of LC3, p62, and Beclin-1 levels in different cell groups. (F) The mRFP-GFP-LC3 fluorescence assay was utilized for assessing autophagic flux. (G) Cell viability was tested by CCK-8 kit. (H) Flow cytometry was utilized for testing cell apoptosis. (I) ELISA was implemented for evaluating the contents of TNF-α, IL-1β, IL-6, and IL-17. **P<0.01.

BMSC-expos on ALI

Cell. Mol. Biol. 2024, 70(2): 104-112

phagy protein levels and autophagy flux (Figures 2E, F). Thus, these discoveries demonstrated that BMSC-expos can promote the autophagy of PMVECs under LPS conditions. Next, we further determined BMSC-exo functions on cell viability, apoptosis, and inflammatory reaction. CCK-8 assay and flow cytometry analysis manifested that cell viability reduced by LPS and cell apoptosis enhanced by LPS were reversed by BMSC-expos treatment, while 3-MA addition can abolish the function of BMSC-expos (Figures 2G, H). Furthermore, LPS-induced high contents of TNF-α, IL-1β, IL-6, and IL-17 in PMVECs were reduced after BMSC-exo treatment, while this decrease can be reversed by 3-MA addition (Figure 2I). Thus, we confirmed that BMSC-expos activated autophagy in PMVECs to alleviate LPS-induced apoptosis and inflammation.

3.3. BMSC-expos increase miR-26a-3p and decrease PTEN in PMVECs

We further investigated the molecular mechanism of BMSC-expos in protecting ALI. Through RT-qPCR outcomes, we discovered miR-26a-3p in supernatant of BMSCs was markedly reduced by GW4869 addition (Figure 3A). Furthermore, miR-26a-3p expression in PMVECs was found to be reduced in the LPS group, elevated in the LPS+BMSC group, and declined in
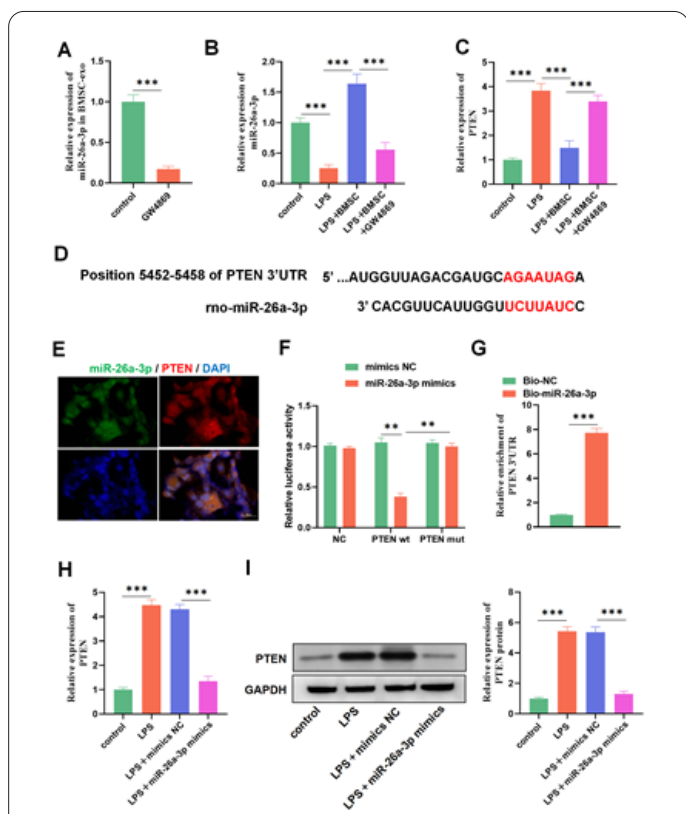
Fig. 3. BMSC-expos increase miR-26a-3p and decrease PTEN in PMVECs. RT-qPCR outcomes of miR-26a-3p in BMSC-expos treated with or without GW4869. (B-C) RT-qPCR outcomes of miR-26a-3p and PTEN expressions in PMVECs of the LPS group, the LPS+BMSC group, and the LPS+BMSC+GW4869 group. (D) The binding site of miR-26a-3p and PTEN 3'UTR was predicted through TargetScan. (E) IF assay was applied to measure the co-localization of miR-26a-3p and PTEN in PMVECs. (F-G) Luciferase reporter assay and RNA pull-down assay were utilized to prove the combination of miR-26a-3p and PTEN. (H-I) RT-qPCR and western blot outcomes of PTEN in LPS-induced PMVECs after miR-26a-3p was overexpressed by miR-26a-3p mimics. **P<0.01.
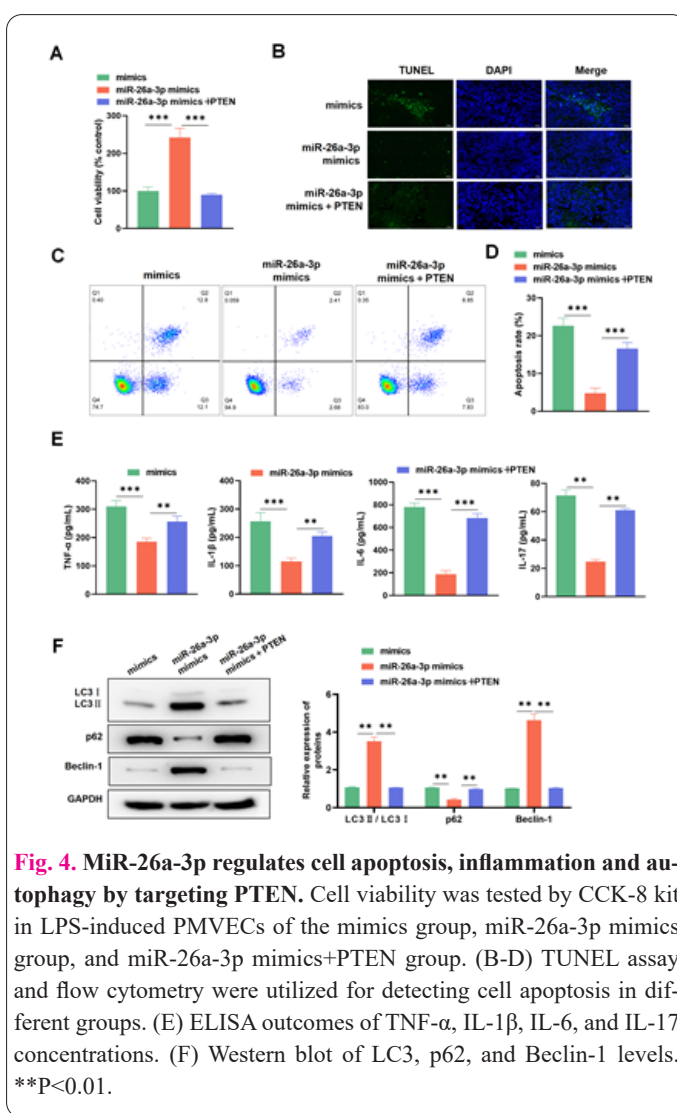
Fig. 4. MiR-26a-3p regulates cell apoptosis, inflammation and autophagy by targeting PTEN. Cell viability was tested by CCK-8 kit in LPS-induced PMVECs of the mimics group, miR-26a-3p mimics group, and miR-26a-3p mimics+PTEN group. (B-D) TUNEL assay and flow cytometry were utilized for detecting cell apoptosis in different groups. (E) ELISA outcomes of TNF-α, IL-1β, IL-6, and IL-17 concentrations. (F) Western blot of LC3, p62, and Beclin-1 levels. **P<0.01.

LPS+BMSC+GW4869 group (Figure 3B). Additionally, we found that PTEN expression in PMVECs showed an opposite trend to that of miR-26a-3p (Figure 3C). Through TargetScan prediction software, we discovered the direct binding sites between miR-26a-3p and PTEN (Figure 3D). IF assay also proved the co-localization of miR-26a-3p and PTEN in PMVECs (Figure 3E). Then we proved that the luciferase activity of PTEN wt was suppressed in miR-26a-3p mimics-transfected cells, which demonstrated that PTEN was a direct target for miR-26a-3p (Figure 3F). Additionally, it was manifested by RNA pull-down assay that the bio-miR-26a-3p probe notably pulled down the enrichment of PTEN in PMVECs (Figure 3G). In addition, PTEN levels in PMVECs enhanced by LPS notably reduced miR-26a-3p overexpression, suggesting the negative regulation between PTEN and miR-26a-3p (Figures 3H, I). Thus, we confirmed that BMSC-expos regulated the miR-26a-3p/PTEN axis in PMVECs.

3.4. MiR-26a-3p modulates cell apoptosis, inflammation and autophagy by targeting PTEN

We further investigated the impacts of the miR-26a-3p/PTEN axis on LPS-induced injury in PMVECs. CCK-8 assay manifested miR-26a-3p mimics notably elevated cell viability, while this increase was abolished by PTEN enhancement (Figure 4A). Then, we proved that PTEN overexpression notably counteracted the suppressive function of miR-26a-3p upregulation on cell apoptosis (Figures

4B-D). ELISA results proved that TNF-α, IL-1β, IL-6, and IL-17 concentrations reduced via miR-26a-3p upregulation can be reversed via PTEN overexpression (Figure 4E). In addition, in the miR-26a-3p overexpressed cells, we observed the increase of LC3II and Beclin-1 as well as the decrease of p62. However, these alterations were all reversed by PTEN overexpression (Figure 4F). Thus, we proved that miR-26a-3p regulated cell apoptosis, inflammation and autophagy by targeting PTEN.

3.5. MiR-26a-3p relieves LPS-induced lung injury in ALI rats

Finally, we further confirmed the functions of miR-26a-3p on ALI *in vitro* by constructing a LPS-induced ALI rat model. Based on survival analysis, we discovered that the survival rate of ALI rats notably declined in comparison to control rats, while ALI rats injected with miR-26a-3p had a longer survival time (Figure 5A). HE staining proved that LPS induction resulted in the notable infiltration of leukocytes, alveolar edema, and septal thickening in lung tissues. Nevertheless, miR-26a-3p treatment alleviated histopathological alterations and reduced the severity of lung injury (Figure 5B). At the same time, miR-26a-3p treatment decreased LPS-induced high score of lung injury (Figure 5C). For evaluating the impacts of miR-26a-3p on pulmonary vascular permeability, we measured the W/D ratio and found that the ratio of ALI rats markedly elevated in comparison of the sham rats. However, this ratio showed a significant decline after miR-26a-3p enhancement (Figure 5D). Furthermore, we discovered that LPS induction elevated the extravasation of Evans blue dye in

Fig. 6. MiR-26a-3p suppresses inflammation and promotes autophagy in LPS-induced ALI rats. (A-H) ELISA outcomes of TNF-α, IL-1β, IL-6, and IL-17 contents in serum and BALF of rats in the sham group, the LPS group, and the LPS+miR-26a-3p group. (I, J) Western blot outcomes of LC3, p62, and Beclin-1 levels in lung tissues. **P<0.01.
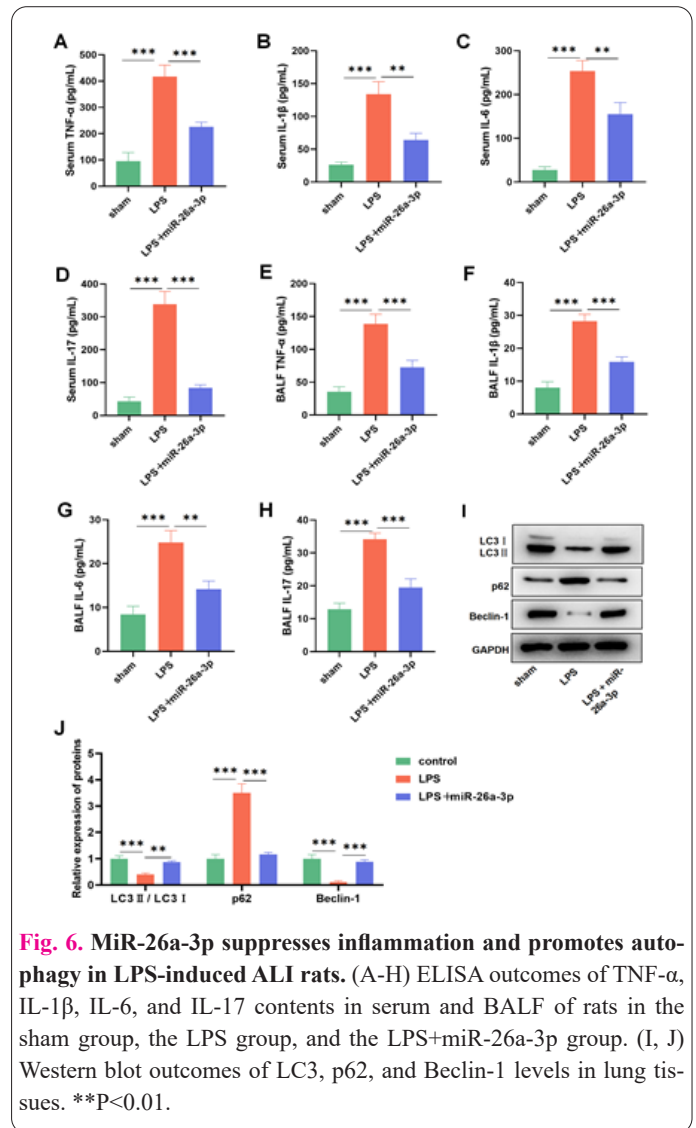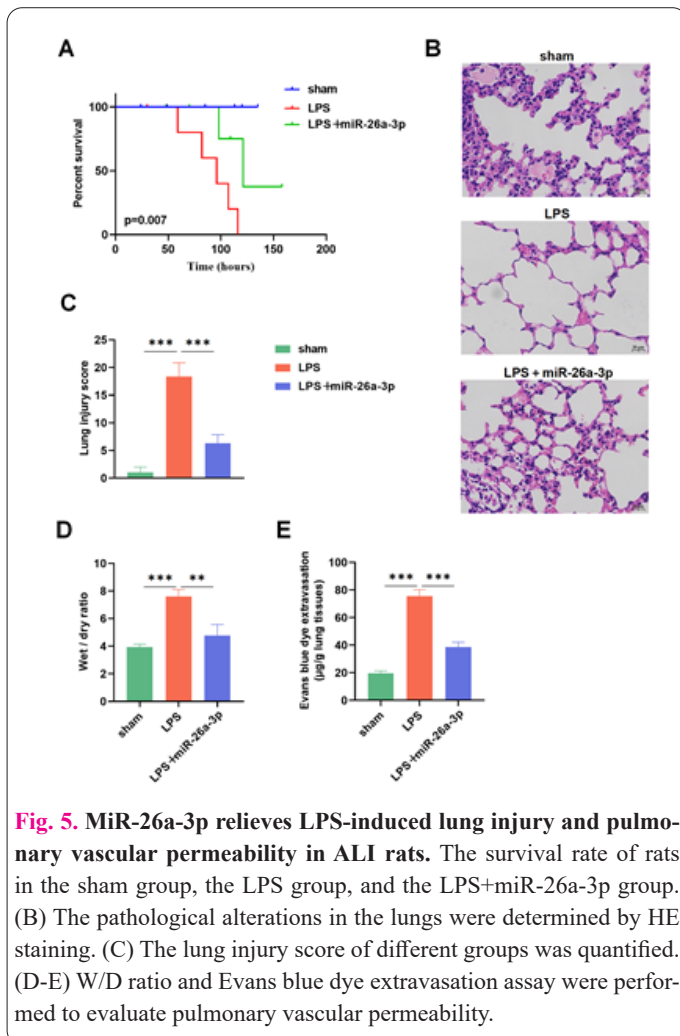
lung tissues, but decreased after miR-26a-3p overexpression (Figure 5E). These discoveries confirmed that miR-26a-3p overexpression effectively improved LPS-induced lung injury and pulmonary vascular permeability.

3.6. MiR-26a-3p suppresses inflammation and promotes autophagy in LPS-induced ALI rats

We further utilized ELISA to measure the impacts of miR-26a-3p on the concentrations of inflammatory factors in serum and BALF of rats. Compared with the sham rats, TNF-α, IL-1β, IL-6, and IL-17 contents in serum and BALF were drastically elevated after LPS stimulation. In contrast, miR-26a-3p injection notably reduced their contents increased by LPS, indicating miR-26a-3p alleviated the inflammatory reaction caused by LPS (Figures 6A-H). Western blot further proved that LPS administration reduced LC3II/LC3I ratio and Beclin-1 levels as well as increased p62 levels, while miR-26a-3p overexpression reversed their levels in lung tissues (Figures 6I, J). Thus, we confirmed that miR-26a-3p suppressed inflammation and promoted autophagy in LPS-induced ALI rats.

4. Discussion

ALI is an inflammatory lung disease caused by multiple factors. However, there is still a lack of effective drugs for treatment. Emerging evidence suggests that microvascular endothelial inflammation and cell apoptosis are the principal causes of ALI [19, 20]. Researches have proved

Fig. 5. MiR-26a-3p relieves LPS-induced lung injury and pulmonary vascular permeability in ALI rats. The survival rate of rats in the sham group, the LPS group, and the LPS+miR-26a-3p group. (B) The pathological alterations in the lungs were determined by HE staining. (C) The lung injury score of different groups was quantified. (D-E) W/D ratio and Evans blue dye extravasation assay were performed to evaluate pulmonary vascular permeability.

BMSC-expos on ALI

Cell. Mol. Biol. 2024, 70(2): 104-112

that LPS can induce the production of pro-inflammatory factors and reactive oxygen species by activating NF-κB inflammatory signal in lungs and BALF, subsequently disrupting the endothelial barrier and resulting in microvascular leakage [21, 22]. Therefore, exploring the molecular mechanisms of LPS-induced apoptosis and inflammatory response in PMVECs is crucial for the treatment of ALI. More and more studies have suggested that exosomes derived from mesenchymal stem cells have been widely studied as a novel strategy for cell-free therapy in different diseases [18, 23, 24]. BMSC-expos are considered a promising strategy for ALI due to their anti-apoptotic, anti-inflammatory, and antioxidant functions. In this study, we discovered that the treatment of BMSC-expos notably elevated the activity of PMVECs suppressed by LPS. In addition, cell apoptosis induced by LPS was reversed by BMSC-expos. It is reported that continuously elevated levels of pro-inflammatory cytokines can highly predict mortality in ALI patients [25, 26]. Herein, we proved that TNF-α, IL-1β, IL-6, and IL-17 concentrations were increased by LPS stimulation in PMVECs, while BMSC-expos reduced the release of these inflammatory factors. These results indicate that BMSC-expos can alleviate LPS-induced damage in PMVECs through anti-apoptotic and anti-inflammatory functions, thereby alleviating ALI progression.

Autophagy is the self-digestion process of cells and takes part in the maintenance of abnormal organelles and macromolecules, ensuring the survival of cells under different pressure conditions [27]. The protective effect of autophagy on cells under physiological conditions involves negative regulation of cell apoptosis. Studies have confirmed that the activation of autophagy exhibits a protective effect during ALI [28]. Castillo *et al*. [29] have suggested that autophagy-deficient mice exhibit stronger inflammation. Autophagy suppression can enhance LPS-induced ALI through the NF-κB pathway [30]. In addition, it is reported that exosomes secreted by MSCs facilitate protective effects via stimulating autophagy in ALI [31]. The LC3II/LC3I ratio is extensively utilized as a biomarker for autophagy. The activation of autophagy is positively associated with the LC3II/LC3I ratio and negatively correlated with P62 expression. Beclin1 exerts a vital function in the formation of autophagosomes. Herein, we proved that BMSC-expos markedly facilitated the formation of autophagosomes, increased the LC3II/LC3I ratio, promoted the Beclin-1 levels, and suppressed p62 levels in LPS-induced PMVECs. In addition, we found that the addition of autophagy inhibitor 3-MA reversed the promoting effect of BMSC-expos on cell activity and the inhibitory effects on cell apoptosis and inflammation. These discoveries indicate that BMSC-expos alleviate LPS-induced cell apoptosis and inflammation by activating autophagy in PMVECs.

Numerous studies have demonstrated that miRNAs in BMSC-expos may be the main reason for their protective effects on damaged tissue repair in different diseases. A large number of miRNAs have been proven to take part in modulating biological functions, many of which have been confirmed to be delivered to receptor cells through exosomes. Therefore, we speculated that certain miRNAs contained in BMSC-expos may be involved in alleviating ALI. MiR-26a-3p is closely related to synaptic formation and plasticity in the nervous system. The involvement and modulation of miR-26a-3p have been found in neurological diseases and some cancers [13, 14, 32]. In addition, studies have indicated that miR-26a-3p can enhance autophagosome/lysosomal activity, facilitate synaptic plasticity, and repress neuronal cell apoptosis [13]. Moreover, miR-26a-3p absence results in an elevation in the expressions of pro-inflammatory factors IL-6β, IL-4, and TNF-α in the injured neurons [14]. Our results discovered that miR-26a-3p expression in BMSCs was reduced via the exosome inhibitor GW4869. In PMVECs, miR-26a-3p expression was suppressed by LPS but notably overexpressed in the co-culture system with BMSCs. MiR-26a-3p upregulation markedly enhanced the levels of autophagy proteins in LPS-induced PMVECs, restrained cell apoptosis and pro-inflammatory factor contents. These findings indicate that exosomal miR-26a-3p improves LPS-induced ALI by reducing cell injury of PMVECs.

PTEN has been identified as a vital tumor suppressor that possesses dual-specific phosphatase [33]. PTEN is a negative regulator of the PI3K/Akt pathway and it modulates assorted biological processes, such as cell proliferation, survival, and metabolism [34]. It is reported that PTEN can stimulate inflammatory reactions via repressing the PI3K pathway in sepsis-induced ALI [35]. The activation of myeloid PTEN facilitates lung inflammation after bacterial infection. Herein, we proved miR-26a-3p combined with PTEN and negatively regulated its expression. PTEN high expression induced by LPS in PMVECs was reversed by BMSC-expos. Overexpression of PTEN notably offset the miR-26a-3p functions on cell apoptosis, inflammation and autophagy in LPS-induced PMVECs. Thus, we prove that BMSC-expos alleviate ALI progression through the miR-26a-3p/PTEN axis.

In the animal experiments, we proved that miR-26a-3p significantly mitigated LPS-induced lung injury and pulmonary vascular permeability. In addition, the concentrations of proinflammatory factors in serum and BALF of ALI rats were reduced by miR-26a-3p. The expressions of autophagy proteins were also decreased by miR-26a-3p. These results strongly confirm the protective effect of miR-26a-3p in LPS-induced ALI.

Taken together, this study proves that BMSC-expos enhance autophagy to reduce LPS-induced cell apoptosis and inflammation in PMVECs through miR-26a-3p/PTEN axis, thereby alleviating ALI progression. These discoveries provide novel therapeutic targets for ALI.

References

1. Long ME, Mallampalli RK, Horowitz JC (2022) Pathogenesis of pneumonia and acute lung injury. Clin Sci (Lond) 136 (10):747–769. doi: 10.1042/cs20210879

2. Zhang K, Wang P, Huang S, Wang X, Li T, Jin Y, et al (2014) Different mechanism of LPS-induced calcium increase in human lung epithelial cell and microvascular endothelial cell: a cell culture study in a model for ARDS. Mol Biol Rep 41(7):4253–4259. doi: 10.1007/s11033-014-3296-1

3. Maldonado RF, Sá-Correia I, Valvano MA (2016) Lipopolysaccharide modification in Gram-negative bacteria during chronic infection. FEMS Microbiol Rev 40(4):480–493. doi: 10.1093/femsre/fuw007

4. Charbord P (2010) Bone marrow mesenchymal stem cells: historical overview and concepts. Hum Gene Ther 21(9):1045–1056. doi: 10.1089/hum.2010.115

5. Kalluri R, LeBleu VS (2020) The biology, function, and biomedical applications of exosomes. Science 367(6478). doi: 10.1126/science.aau6977

6. Familtseva A, Jeremic N, Tyagi SC (2019) Exosomes: cell-created drug delivery systems. Mol Cell Biochem 459(1-2):1–6. doi: 10.1007/s11010-019-03545-4

7. Wan R, Hussain A, Behfar A, Moran SL, Zhao C (2022) The therapeutic potential of exosomes in soft tissue repair and regeneration. Int J Mol Sci 23(7):3869. doi: 10.3390/ijms23073869

8. Hade MD, Suire CN, Suo Z (2021) Mesenchymal stem cell-derived exosomes: applications in regenerative medicine. Cells 10(8):1959. doi: 10.3390/cells10081959

9. Liu X, Gao C, Wang Y, Niu L, Jiang S, Pan S (2021) BMSC-derived exosomes ameliorate LPS-induced acute lung injury by miR-384-5p-controlled alveolar macrophage autophagy. Oxid Med Cell Longev 2021:9973457. doi: 10.1155/2021/9973457

10. Mohr AM, Mott JL (2015) Overview of microRNA biology. Semin Liver Dis 35(1):3–11. doi: 10.1055/s-0034-1397344

11. Cui Y, Wang X, Lin F, Li W, Zhao Y, Zhu F, et al (2022) MiR-29a-3p improves acute lung injury by reducing alveolar epithelial cell PANoptosis. Aging Dis 13(3):899–909. doi: 10.14336/ad.2021.1023

12. Yang J, Do-Umehara HC, Zhang Q, Wang H, Hou C, Dong H, et al (2021) miR-221-5p-mediated downregulation of JNK2 aggravates acute lung injury. Front Immunol 12:700933. doi: 10.3389/fimmu.2021.700933

13. Li Y, Fan C, Wang L, Lan T, Gao R, Wang W, Yu SY (2021) MicroRNA-26a-3p rescues depression-like behaviors in male rats via preventing hippocampal neuronal anomalies. J Clin Invest 131(16):e148853. doi: 10.1172/jci148853

14. Wang C, Li Y, Yi Y, Liu G, Guo R, Wang L, et al (2022) Hippocampal microRNA-26a-3p deficit contributes to neuroinflammation and behavioral disorders via p38 MAPK signaling pathway in rats. J Neuroinflammation 19(1):283. doi: 10.1186/s12974-022-02645-1

15. Si Z, Yu L, Jing H, Wu L, Wang X (2021) Oncogenic lncRNA ZNF561-AS1 is essential for colorectal cancer proliferation and survival through regulation of miR-26a-3p/miR-128-5p-SRSF6 axis. J Exp Clin Cancer Res 40(1):78. doi: 10.1186/s13046-021-01882-1

16. Zhang J, Li S, Li L, Li M, Guo C, Yao J, Mi S (2015) Exosome and exosomal microRNA: trafficking, sorting, and function. Genomics Proteomics Bioinformatics 13(1):17–24. doi: 10.1016/j.gpb.2015.02.001

17. Xu J, Xu D, Yu Z, Fu Z, Lv Z, Meng L, Zhao X (2022) Exosomal miR-150 partially attenuated acute lung injury by mediating microvascular endothelial cells and MAPK pathway. Biosci Rep 42(1):BSR20203363. doi: 10.1042/bsr20203363

18. Harrell CR, Jovicic N, Djonov V, Arsenijevic N, Volarevic V (2019) Mesenchymal stem cell-derived exosomes and other extracellular vesicles as new remedies in the therapy of inflammatory diseases. Cells 8(12):1605. doi: 10.3390/cells8121605

19. Cen M, Ouyang W, Zhang W, Yang L, Lin X, Dai M, et al (2021) MitoQ protects against hyperpermeability of endothelium barrier in acute lung injury via a Nrf2-dependent mechanism. Redox Biol 41:101936. doi: 10.1016/j.redox.2021.101936

20. Ren Y, Li L, Wang MM, Cao LP, Sun ZR, Yang ZZ, et al (2021) Pravastatin attenuates sepsis-induced acute lung injury through decreasing pulmonary microvascular permeability via inhibition of Cav-1/eNOS pathway. Int Immunopharmacol 100:108077. doi: 10.1016/j.intimp.2021.108077

21. Tanaka A, Jin Y, Lee SJ, Zhang M, Kim HP, Stolz DB, et al (2012) Hyperoxia-induced LC3B interacts with the Fas apoptotic pathway in epithelial cell death. Am J Respir Cell Mol Biol 46(4):507–514. doi: 10.1165/rcmb.2009-0415OC

22. He M, Shi W, Yu M, Li X, Xu J, Zhu J, et al (2019) Nicorandil attenuates LPS-induced acute lung injury by pulmonary endothelial cell protection via NF-κB and MAPK pathways. Oxid Med Cell Longev 2019:4957646. doi: 10.1155/2019/4957646

23. Yu B, Zhang X, Li X (2014) Exosomes derived from mesenchymal stem cells. Int J Mol Sci 15(3):4142–4157. doi: 10.3390/ijms15034142

24. Yaghoubi Y, Movassaghpour A, Zamani M, Talebi M, Mehdizadeh A, Yousefi M (2019) Human umbilical cord mesenchymal stem cells derived-exosomes in diseases treatment. Life Sci 233:116733. doi: 10.1016/j.lfs.2019.116733

25. Meduri GU, Kohler G, Headley S, Tolley E, Stentz F, Postlethwaite A (1995) Inflammatory cytokines in the BAL of patients with ARDS. Persistent elevation over time predicts poor outcome. Chest 108(5):1303–1314. doi: 10.1378/chest.108.5.1303

26. Parsons PE, Eisner MD, Thompson BT, Matthay MA, Ancukiewicz M, Bernard GR, Wheeler AP (2005) Lower tidal volume ventilation and plasma cytokine markers of inflammation in patients with acute lung injury. Crit Care Med 33(1):1-6; discussion 230–232. doi: 10.1097/01.ccm.0000149854.61192.dc

27. Glick D, Barth S, Macleod KF (2010) Autophagy: cellular and molecular mechanisms. J Pathol 221(1):3–12. doi: 10.1002/path.2697

28. Junkins RD, Shen A, Rosen K, McCormick C, Lin TJ (2013) Autophagy enhances bacterial clearance during P. aeruginosa lung infection. PLoS One 8(8):e72263. doi: 10.1371/journal.pone.0072263

29. Castillo EF, Dekonenko A, Arko-Mensah J, Mandell MA, Dupont N, Jiang S, et al (2012) Autophagy protects against active tuberculosis by suppressing bacterial burden and inflammation. Proc Natl Acad Sci U S A 109(46): E3168–3176. doi: 10.1073/pnas.1210500109

30. Hu Y, Lou J, Mao YY, Lai TW, Liu LY, Zhu C, et al (2016) Activation of MTOR in pulmonary epithelium promotes LPS-induced acute lung injury. Autophagy 12(12):2286–2299. doi: 10.1080/15548627.2016.1230584

31. Wei X, Yi X, Lv H, Sui X, Lu P, Li L, et al (2020) MicroRNA-377-3p released by mesenchymal stem cell exosomes ameliorates lipopolysaccharide-induced acute lung injury by targeting RPTOR to induce autophagy. Cell Death Dis 11(8):657. doi: 10.1038/s41419-020-02857-4

32. Ye MF, Lin D, Li WJ, Xu HP, Zhang J (2020) MiR-26a-5p serves as an oncogenic microRNA in non-small cell lung cancer by targeting FAF1. Cancer Manag Res 12:7131–7142. doi: 10.2147/cmar.S261131

33. Chen CY, Chen J, He L, Stiles BL (2018) PTEN: Tumor Suppres-

BMSC-expos on ALI

Cell. Mol. Biol. 2024, 70(2): 104-112

sor and Metabolic Regulator. Front Endocrinol (Lausanne) 9:338. doi: 10.3389/fendo.2018.00338

34. Mukherjee R, Vanaja KG, Boyer JA, Gadal S, Solomon H, Chandarlapaty S, et al (2021) Regulation of PTEN translation by PI3K signaling maintains pathway homeostasis. Mol Cell 81(4):708–723.e705. doi: 10.1016/j.molcel.2021.01.033

35. Zhou M, Fang H, Du M, Li C, Tang R, Liu H, et al (2019) The modulation of regulatory T cells via HMGB1/PTEN/β-catenin axis in LPS induced acute lung injury. Front Immunol 10:1612. doi: 10.3389/fimmu.2019.01612